Ultracold Hydrogen

Lorenz Willmann and Daniel Kleppner

Massachusetts Institute of Technology,
Department of Physics, Cambridge, MA 02139, USA

Abstract. Scientific interest in ultracold hydrogen arises from its properties as a Bose-Einstein condensate, its unique roles as a testing ground for atomic theory and a target for ultra high resolution spectroscopy. We describe major developments since the last hydrogen meeting.

1 Introduction

In the twelve years since the meeting *The Hydrogen Atom* [1] (now known as H-1) there have been dramatic advances in the field of ultracold trapped hydrogen. The primary goal, the quest for Bose-Einstein condensation (BEC) in hydrogen [2], has been achieved, and the foundations have been laid for ultrahigh resolution spectroscopy of hydrogen with applications to atomic theory- including both fundamental structure and atomic interactions- and to a possible optical frequency standard.

The traditional technique for monitoring trapped hydrogen– monitoring the flux of atoms dumped from a trap by the recombination energy deposited on a bolometer – is poorly suited to searching for BEC. At H-1 a new technique was described based on 1S-2S two-photon spectroscopy. The Doppler sensitive signal from absorption of two co-propagating photons reveals the momentum distribution of the atoms, while the narrow Doppler free signal, from absorption of counter-propagating photons, provides a strong calibration signal, and can reveal small perturbations. Work on this commenced in 1989 and some years later the two-photon signal was observed. [3].

With the new “eyes” of two-photon spectroscopy we continued toward BEC, but discovered that at low temperatures the evaporation lost efficiency. The atoms are trapped in a long Ioffe-Pritchard trap and allowed to escape by lowering the confining field at one end of the trap (”saddle-point evaporation”). The fall in efficiency was analyzed by Surkov et al. [4]. They showed that mixing of radial and longitudinal motion decreases at low energy, causing the total energy flow to be blocked. One possible solution to the problem is to release the atoms optically over a larger effective area, using a Zeeman-sensitive Lyman-α transition. Furthermore, the Lyman-α transition can also be used for laser-cooling. Temperatures of a few millikelvin were achieved by that technique [5]. However, due to limitations of Lyman-α sources, the method could not fully overcome the cooling problem.

To overcome the limitations of saddle-point evaporation, we finally implemented the method which had been standard in all BEC experiments. This is

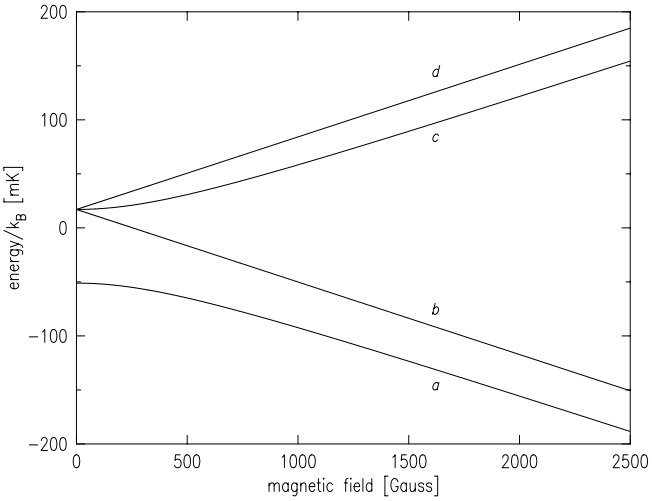

Fig. 1. Hyperfine diagram for the ground state of atomic hydrogen. The 'high field seeking' states a and b can be stabilized in a high magnetic field, while the 'low field seeking' states c and d are trapped in the minimum of a magnetic field

"rf evaporation" [7], in which a Zeeman transition to a non-trapped state is induced by an applied rf field. Because the atoms escape over the entire surface where the resonance condition is met, the evaporation is fully three dimensional.

Implementing rf evaporation required an apparatus redesign, but the method opened the way to rapid progress. The atomic density grew to the point that the cold-collision frequency shift of the 1S-2S transition became visible [8], providing an *in situ* measurement of the density. With this tool, the BEC transition was soon achieved [9]. We shall describe our BEC studies below.

The antecedent of ultracold hydrogen is spin-polarized hydrogen in which atoms in the high field seeking states (states a and b in Fig. 1) are confined in a liquid helium coated cell. As described in a review article by Walraven, [10], the hydrogen-helium system provides is close to ideal for studying atom-surface interactions, including the phenomenon of quantum reflection [11]. Furthermore, the gas phase of a spin-polarized hydrogen system is in equilibrium with a quasi two dimensional phase in which the surface density can approach quantum degeneracy. Observation of quantum effects have been reported by [12,13,14].

To return to optical studies, two-photon Doppler-free spectroscopy of the 1S-2S transition in hydrogen is technically challenging because of its small transition amplitude. This problem can be ameliorated by employing resonance enhanced two-photon spectroscopy of the 1S-3D/3S transition [15], using 122 nm and 656 nm radiation. The transition rate is enhanced by tuning the Lyman-α source close to resonance. With a narrow bandwidth Lyman-α source this scheme is potentially useful for studying the momentum distribution, and determining the temperature, using Doppler spectroscopy.

As described in H-I, ultracold hydrogen has great potential for ultrahigh resolution spectroscopy of hydrogen [16]. In particular, it holds the promise of providing a resolution close to the natural linewidth, 1.3 Hz. As documented by presentations at this conference, this transition is a touchstone for spectroscopy, studies of fundamental theory and determination of fundamental constants [17].

Since the conference H-1, progress in the study of the 1S-2S transition has been spectacular. In particular, one of the most precise measurements of an optical transition has been achieved with this transition, using a cooled hydrogen beam [18]. Nevertheless, the spectral resolution so far achieved is about three orders of magnitude larger than the natural linewidth, so that significant improvements are still possible. The lifetime of the 2S state in a gas of ultracold hydrogen has been observed to be essentially the natural lifetime [3], which suggests that a resolution comparable to the natural linewidth can one day be achieved.

In order to extract the QED or nuclear effects from the 1S-2S frequency, a second frequency must be known. The present uncertainty in the Lamb shift and Rydberg constant is determined by the accuracy of such a measurement. The most precise measurements have been made on transitions from 2S to higher levels in a super-thermal beam of metastable 2S atoms [19]. As will be described, ultracold hydrogen offers possibilities for significant improvements.

The enormous difficulty of making optical frequency measurements has been a major obstacle to progress. The optical frequency comb generator devised by Hänsch overcomes these difficulties, and promises to revolutionize spectroscopy. The technique, based upon a mode-locked laser, makes it possible to connect microwave and optical frequencies, or to determine relative optical frequencies [20,21]. In particular, it allows to transport the stability of optical transitions into the microwave frequency range. A report by J. Hall about these developments can be found in these proceedings.

Finally, we note that ultracold hydrogen holds enormous potential for the study of atomic interactions. For instance, scattering lengths can be determined directly from spectral line shifts [8]. Furthermore, photoassociation spectroscopy can be used to investigate the potentials for excited H_2 potentials, as in a recent investigation of the molecular triplet $a^3\Sigma_g^+$ potential [13].

In the following we will describe work on ultracold hydrogen at MIT, and suggest some of the new opportunities.

2 Ultracold Hydrogen Research at MIT

2.1 The Road to Bose-Einstein Condensation

Trapping and Cooling

With only one exception, every experiment on BEC has employed laser cooling and trapping methods to create a gas of cold atoms. The exception is hydrogen. The recoil energy of hydrogen is so large that the gas cannot be cooled below a few millikelvin, with densities far from the transition. (The Amsterdam group

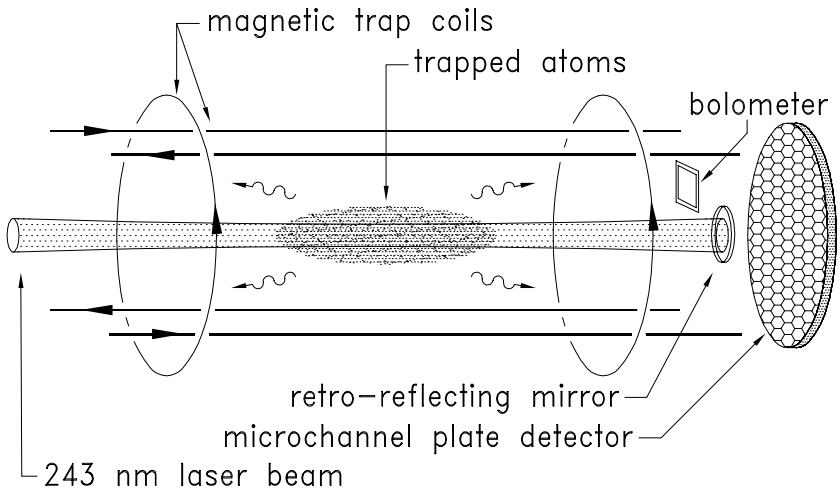

Fig. 2. Schematic diagram of the apparatus. The superconducting magnetic coils create trapping potential that confines atoms near the focus of the 243 nm laser beam. The beam is focused to a 50 μm waist radius and retro-reflected to allow for Doppler-free excitation. After excitation, fluorescence is induced by an applied electric field. A small fraction of the 122 nm fluorescence photons are counted on a microchannel plate detector. Not shown is the trapping cell which surrounds the sample and is thermally anchored to a dilution refrigerator. The actual trap is longer and narrower than indicated in the diagram

has actually demonstrated laser cooling into this regime [5]. Consequently, evaporative cooling [22]. is used exclusively for trapping the gas and cooling it to the quantum transition. Only with hydrogen is such an approach possible. A magnetic trap can only capture atoms in the sub-Kelvin regime, and only hydrogen can be initially cooled to sub-Kelvin temperatures by cryogenic methods. If the atoms are spin-polarized, they can be thermalized in this regime simply by colliding with a liquid helium surface. (The binding energy is 1K, which is anomalously low.) This fact, added to the recognition that spin-polarized hydrogen remains a gas to T=0, inspired the initial search for BEC in an atomic gas [23].

Atoms are provided from an rf discharge source, at cryogenic temperatures. After thermalization on the cold cell walls, typically 250 mK, the "low field seeking" states, c and d (Fig. 1) are attracted to the center of a Ioffe-Pritchard trap, a linear quadrupole trap with a coil at each end to confine the atoms axially. The trapping field is initially about 0.9 T, sufficient to capture atoms with a temperature of about 0.5 K. Once the temperature of the walls is reduced, the temperature of the trapped gas rapidly falls by evaporation, the escaping atoms being trapped on the helium surface. At about 60 mK, the gas becomes isolated from the wall and evaporation ceases.

Dipolar Decay and Density Measurement

The stability of the trapped gas is a crucial factor in the subsequent cooling scenario. Both the c and d states can be transferred to lower lying hyperfine states through collisions, and lost from the trap. The c state decays quickly by spin-exchange collisions. However, d state collisions occur in a pure triplet molecular potential, and there is no spin exchange. Nevertheless, the atoms can move to lower-lying states by the process of dipole relaxation. In this process, the electronic spin-spin interaction causes internal spin angular momentum to be transformed into external orbital angular momentum, transferring potential energy into kinetic energy. Dipole relaxation is the principal mechanism by which atoms are lost from the trap, causing the sample to decay by two-body relaxation.

The density and the number of trapped atoms can be inferred from the decay of the sample. Atoms are dumped from the trap by lowering one of the axial confining fields. The emerging atoms recombine rapidly on the walls of the cell, releasing an energy of 4.6 eV per recombination. A fraction of this energy is collected on a small quartz bolometer [24]. The total integrated power is proportional to the total number of atoms in the trap.

The sample decay curve, $N(t)$, is obtained by measuring the number of trapped atoms after various holding times. The local decay n decreases due to dipolar decay according to $\dot{n} = -gn^2$, were $g = 1.1 \times 10^{15}\mathrm{cm}^3/s$ is the dipolar decay constant, which is known from measurements [25,26] and theory [27,28]. Integration over the trap volume yields $\dot{N} = -\kappa g N^2$, where $\kappa \approx 0.2$ results from the distribution of densities. The result is $N(t)/N(0) = 1/(1+\kappa g n_0 t)$, thus determining the peak density n_0 (Fig. 3). Typically, at a density of 10^{14} cm^{-3}

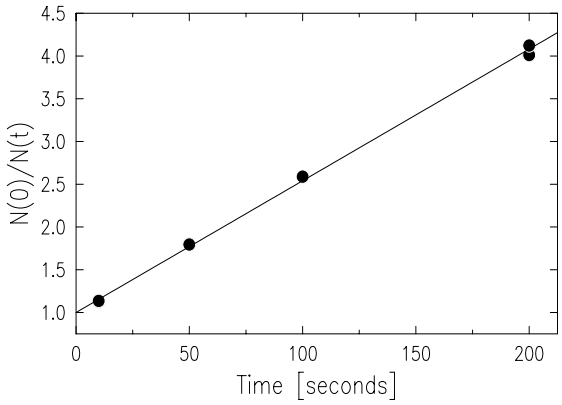

Fig. 3. Determination of the sample density by observing decay due to dipolar relaxation. Five identically prepared samples were held for different times before being dumped from the trap. The integrated recombination signal on a bolometer is proportional to the number of atoms trapped. The straight line fit indicates a density of $6.0 \cdot 10^{13}$ cm^{-3}. There is a 20 % error on the density determination due to the uncertainty in g

the characteristic decay time is 40 s. Using the known geometry of the trapping field, the number of trapped atoms can be found from n_0. Typically, we load 10^{14} atoms at 40 mK. After evaporative cooling to 100 μK, the number of atoms is about 10^{11}.

Limits of Evaporative Cooling

Initially the atoms are evporatively cooled by lowering the magnetic field strength at one end of the trap, thus reducing the trap depth. This method becomes inefficient at about 100 μK when atoms promoted to high-energy states have a high probability of undergoing a collision before escaping from the end of the trap. Temperatures of 100 μK at densities of 8×10^{13} cm^{-3} were achievable [6] but the Bose-Einstein phase transition line could not be crossed. The dynamics are discussed in detail by Surkov et al. [4]. In principle this merely retards the cooling process, but in the presence of a loss mechanism such as dipolar decay, it limits the minimum attainable temperature.

A solution to this problem is the use of rf induced hyperfine transitions [7] to release atoms from the trap. The rf frequency is tuned to be in resonance with a particular magnetic field, B_e. Because the trap potential $V(B)$ is proportional to B, only atoms with energy equal to $V(B_e)$ can escape. Consequently, all the atoms that pass across the potential energy surface $V(B_e)$ can leave. this process, inherently three-dimensional, is much more efficient than the one dimensional evaporation over a saddle-point at the end of a long and thin trap. Implementing rf evaporation into the cryogenic apparatus was a crucial step in achieving BEC of hydrogen.

2.2 Two-Photon 1S-2S Spectroscopy

To witness BEC a more sensitive probe of the gas is needed than the relatively crude bolometric method described above. Direct spatial imaging of the atoms with a CCD camera, widely used in experiments with alkali metal atoms, is impractical because of the lack of VUV optics and light sources. High resolution spectroscopy of the 1S-2S transition, however, provides an excellent diagnostic tool for ultracold trapped hydrogen. Excitation takes place in a standing light wave tuned to one-half the transition frequency. Both Doppler-free and Doppler-sensitive excitation can be observed. The density can be found from the the cold collision frequency shift [8] of the narrow Doppler-free excitation line, and the temperature can be deduced from the width of the Doppler-free transition at low density [3] or the broadening of the Doppler-sensitive absorption line [9].

Laser System

To provide the 243 nm radiation needed for the 1S-2S transition, a laser at 486 nm is stabilized to a reference cavity that reduces the linewidth to less than 1 kHz. The frequency is doubled in a BBO-crystal to produce 243 nm radiation.

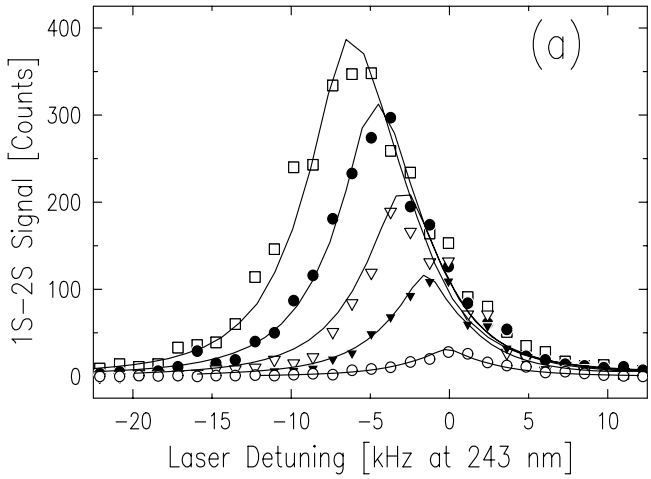

Fig. 4. Cold collision frequency shift observed in the spectra of a single 120 μK sample with initial maximum density of 6.6×10^{13} cm^3. The farthest red shifted spectrum corresponds to the largest density

The laser beam is introduced parallel to the axis of the trap and retro-reflected by a mirror at the bottom of the trapping cell (Fig. 2.) A mechanical chopper pulses the laser at typically 1 kHz. The 2S atoms are in the same hyperfine state d and therefore remain trapped. After excitation for a brief period, the population of the 2S level is measured by detecting the Lyman-α fluorescence in an applied electric field. A microchannel plate detector is used to permit single photon detection. Due to the small optical collection efficiency for our geometry, the detection efficiency is limited to 10^{-5}. Nevertheless, signal rates as high a few hundred thousand counts per second laser time have been observed.

At low density ($< 10^{12}$ cm^{-3}) and temperatures > 100 μK the two-photon lineshape is a double exponential, exp(-$|\nu|/\delta\nu_o$) [3], as expected for Doppler-free two-photon excitation by a Gaussian laser beam of a thermal gas [29]. Here ν is the laser detuning from resonance and $\delta\nu_o$ is the linewidth due to the finite interaction time of the atom with the laser beam. At low temperature, lines as narrow as 3 kHz (FWHM at 243 nm) have been observed. A detailed discussion of this lineshape in the trap and the appearance of sidebands due to coherence effects for repeated crossing of the laser beam can be found in [30].

Cold Collision Frequency Shift

Interactions between neighboring atoms shift and broaden the line. This can be described from a many-body picture as a result of the mean field energy shift, $\Delta E_e = (4\pi\hbar^2 a_{e,g}/m)\, n_g$, where $a_{e,g}$ is the s-wave scattering length of atoms in state e and g, m is the atomic mass, and n_g is the density of g-state atoms. From the an atomic standpoint it is equal to a cold collision frequency shift which we

get as the sum of the mean field shifts of the atomic states involved, when we sum over all partial densities. For the hydrogen 1S-2S transition this is simple since the most of the atoms remain in the 1S state.

The cold collision frequency shift is important in precision frequency measurements and has been observed in hydrogen maser [31] and fountain clock [32,33] experiments. From the point of view of precision measurements, the cold collision shift is an obstacle. However, in BEC experiments, the shift provides a helpful diagnostic for the density.

For hydrogen, the 1S-1S interaction is extremely small and the 1S-2S interaction is the dominant source of the observed frequency shift (Fig. 4). We have measured a_{1S-2S}=-1.4(3) nm [8], which is in fair agreement with a theoretical calculation of a_{1S-2S}=-2.3 nm [34]. We use this shift for measuring the density of the sample on our way to the Bose-Einstein phase transition.

2.3 Bose-Einstein Condensation

We recall that Bose-Einstein condensation is the macroscopic occupation of the ground state of a system at finite temperature. For a weakly interacting gas, this phase transition occurs when the inter-particle spacing becomes comparable to the thermal de Broglie wavelength $\Lambda = \sqrt{2\pi\hbar^2/mk_BT}$, where k_B is the Boltzmann constant and T is the temperature. A rigorous treatment for the ideal Bose gas yields $n \geq 2.612\Lambda^{-3}$, where n is the density [35]. At a temperature of 50 μK, for instance, the critical density for hydrogen is $1.8 \times 10^{14} cm^3$.

Bose-Einstein condensation of an atomic gas was achieved first with alkalide metal atoms [36]. The experiments employed laser cooling and trapping techniques. However, the initial search for BEC in a dilute atomic gas was done with spin-polarized hydrogen, and was motivated by the realization that only hydrogen would remain a gas at zero temperature [23]. Now it is understood that laser cooling allows to cool atoms to temperatures for which they would form a solid in thermal equilibrium, but the relaxation time into the ground state is far longer than the time required to cool the atoms below the critical temperature for the Bose-Einstein transition. The early experiments with hydrogen employed the high field seeking states where the atoms were confined in a helium coated cell at low temperatures. A review of this work can be found in [2].

An overview on the vast experimental and theoretical work on BEC recently we refer to the BEC-homepage [37]. Most experimental BEC research is carried out with alkali metal atoms and the main topics are to characterize the quantum fluid.

The fundamental differences between hydrogen and the other condensed species arise from its low mass, which allows a higher critical temperature for a given density, and its anomalously small elastic scattering cross section $\sigma = 4\pi a_{1S-1S}^2 = 0.053$ nm^2, which limits the evaporative cooling rate. The low cooling rate limits both the ultimate temperature and the condensate fraction [38]. (The elastic cross sections for the alkali metal atoms are typically larger by a factor of 10^3 to 10^4. Another difference is that the ratio of scattering length to de Broglie wavelength a/Λ. It is much smaller for hydrogen than the alkali

metal atoms. This ratio is often used as a perturbation parameter that describe departures of a Bose-condensate from ideal behavior.

Signatures of Bose-Einstein Condensation

The two-photon spectroscopy described above had made it possible to study three characteristic features of Bose-Einstein condensation: condensation in real space, condensation in momentum space (Fig. 5) and the mapping the phase boundary (Fig. 6) [9].

When the transition temperature is achieved, a finite fraction of the atoms fall into the lowest energy quantum state of the trap. The spatial extent of the condensate is much smaller than the thermal radius of the cloud. Only a small fraction of the atoms are required to create a narrow region of very high density at the bottom of the trap. This high density region is readily observed because of its large cold collision frequency shift. The spectrum arising from the condensate can be seen in (Fig. 5), red-shifted up to 0.5 MHz from the Doppler free line.

The shape of the spectrum is determined by the density distribution in the condensate [39,40]. The ratio of the signal strength of the condensed and the noncondensed part allows us to estimate a condensate fraction of a few percent in agreement with predictions from a balance between evaporative cooling and heating due to dipolar decay [38]. The condensate population is about 10^9 atoms.

The Doppler-sensitive two-photon spectrum of hydrogen is normally undetectable due to the combination of weak excitation rate and broad linewidth. However, at very low temperature the line is narrow enough to be visible. In Doppler-sensitive excitation the atom absorbs two photons moving in the same direction. Consequently, the spectrum is shifted by the photon recoil energy, $(h\nu)^2/4mc^2 = h \times 6.697$ MHz (as measured at 243 nm). The shape of the spectrum is Gaussian (except near the transition, where it is determined by the Bose distribution) with width of $\sqrt{k_B T\ k^2/2\pi^2 m}$, where k is the wave vector of the laser beam. A measurement of the linewidth yields the temperature. The minimum temperature in optical cooling is generally limited by the recoil energy. As can be seen in Fig. 5, however, the Doppler width of the evaporatively cooled hydrogen sample is significantly less than the recoil limit.

The Doppler-sensitive line gives a second clear signature for Bose-Einstein condensation. Because the lowest energy state is the lowest momentum state, the condensate appears as a relatively narrow peak at the center of the Gaussian spectrum. Its width is given by the cold collision frequency shift and is the same as in the case of Doppler free spectrum.

Because of the large density contrast between the condensed and noncondensed fraction, we are able to study the density of the noncondensed fraction even in the presence of the condensate. We determine the peak density from the cold collision shift of the Doppler free line. Reducing the trap depth by lowering the rf-frequency reduces the temperature while increasing the density. However, when the critical density is achieved, as observed by the onset of the far red-shifted signal, the peak density in the noncondensed cloud decreases with

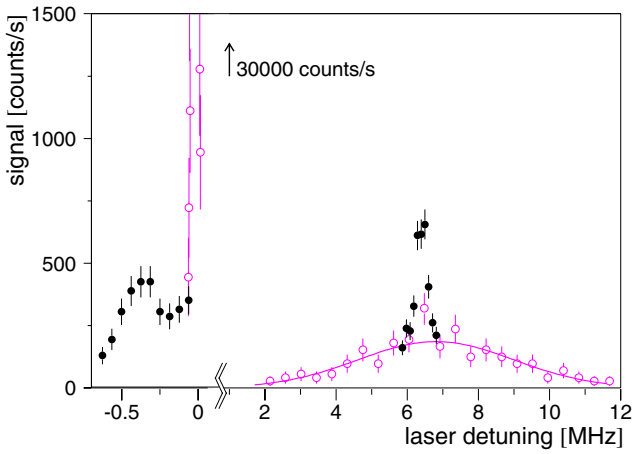

Fig. 5. Composite $1S$-$2S$ two-photon spectrum of trapped hydrogen after condensation. ○–spectrum of sample without a condensate; ●–spectrum emphasizing features due to a condensate. The high density in the condensate shifts a portion of the Doppler-free line to the red. The condensate's narrow momentum distribution gives rise to a similar feature near the center of the Doppler-sensitive line

decreasing temperature (Fig. 6). The density follows the phase boundary predicted by the theory of the transition. No bosonic thermal gas at can exist at densities higher than boundary.

Current experimental efforts at MIT are focused on the dynamics of the growth and decay of the condensate. The dynamics are governed by the balance between evaporation and dipolar decay, mainly from the dense condensate [41]. Condensate growth has been observed with a Na condensate [42]. Because of hydrogen's small elastic scattering cross section, condensation takes place in what might be described as slow motion [44], and the system seems to be well suited for testing theory [43].

2.4 High Resolution Spectroscopy in Ultracold Hydrogen

There are two lines of interest in the spectroscopy of ultracold hydrogen. The first is in the precise determination of the 1S-2S transition frequency. The second is in the many new opportunities made possible by exciting ultracold atoms from the 2S state to higher states.

1S-2S Transition

The 1S-2S transition frequency is so well known [18] that further precision at this time will not yield a better value for the Lamb shift and nuclear shape corrections. Nevertheless, further precision is desirable both for advancing the frontier of optical metrology, and because the transition has potential applications for

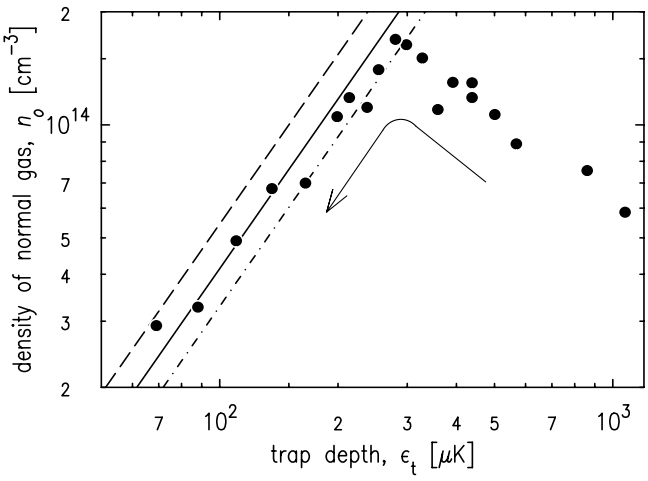

Fig. 6. Density of non-condensed fraction of the gas as the trap depth is reduced along the cooling path. The density is measured by the optical resonance shift, and the trap depth is set by the rf frequency. The lines (dash, solid, dot-dash) indicate the BEC phase transition line, assuming a sample temperature of (1/5th, 1/6th, 1/7th) the trap depth. The scatter of the data reflects the reproducibility of the laser probe technique and is dominated by alignment of the laser beam to the sample

an optical frequency standard. As mentioned above, the experimental resolution achieved with a cooled atomic beam is far short of the ultimate resolution permitted by the natural linewidth. Thus, major improvements are possible.

The major advantage of ultracold trapped hydrogen is that one may be able to achieve a coherence time comparable with the natural lifetime, 122 ms. As described in H-1, [16], The magnetic trapping fields can be reduced to a level where the residual Zeeman shift of the transition is on the order of the natural linewidth of 1.3 Hz. The light-induced shift and the photoionization rate can be reduced to the same level.

It is now recognized that cold collision frequency shifts [32] is a crucial issue for every high precision atomic frequency standard, microwave or optical. For hydrogen at a density of 10^9 cm^{-3} the shift of the 1S-2S transition is about 0.4 Hz, [8], or a fractional shift of 1.7×10^{-16}. For a rubidium hyperfine standard operating at the same density, the shift is about 6×10^{-14} [45,46].

Ultrahigh resolution spectroscopy requires ultrastable lasers. Fortunately, there has been major progress in this areas. A laser locked to an external reference cavity [47] has yielded a resolution of a few parts in 10^{15} for an Hg^+ ion in a trap [48].

2S-nS Transitions

The spectrum of hydrogen is composed of a major structure, determined by the Rydberg constant, QED corrections like the Lamb shift and finally nuclear shape

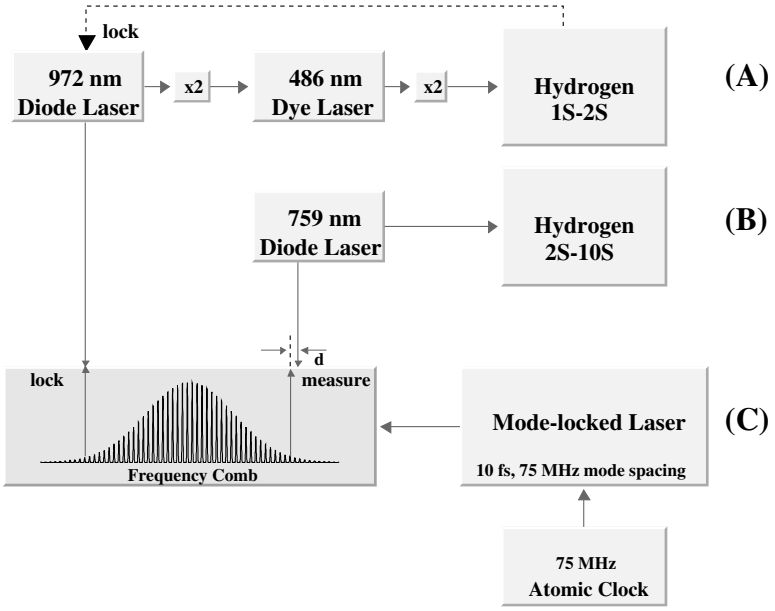

Fig. 7. Possible setup for a frequency measurement of the 2S-10S transition relative to the 1S-2S transition utilizing the new developments with frequency comb generation by mode locked lasers. The measurements are done at the same time in the same trap. The 1S-2S transition is used as the frequency reference (A). The 2S-10S transition is driven by a diode laser (B). The frequency difference between $\nu_{1S-2S}/8$ and $\nu_{2S-10S}/2$ is measured with the help of an optical comb. The scheme can be applied to other 2S-nS transitions as well

contributions. More than two transitions must be measured to unscramble these contributions. The 1S-2S transition, which is most sensitive to the nuclear effect, measured by the Munich group provides one of these. However, the ultimate precision is limited by the second transition, currently one of the two-photon 2S-nS/nD, n=8, 10, 12, transitions that have been studied extensively by the Paris group since the mid 80's [17,19]. These experiments employ a metastable hydrogen beam. The accuracy is about 8×10^{-12} or 5 kHz. Cold trapped hydrogen holds the potential for improving the accuracy of two-photon 2S-nS transitions by an order of magnitude.

We want to outline such an experiment. The precision of the metastable atomic beam experiments is fundamentally determined by the short interaction

time of the metastable atoms. For a beam of length 0.6 m and a mean velocity of the atoms of 3000 m/s the interaction time is only about 200 μs. An efficient excitation rate requires laser intensities of typically 5 kW/cm^2. This intensity causes AC-Stark shifts of a few hundred kHz. The accuracy of the measurement is limited by uncertainty in this shift.

Because ultracold trapped 2S atoms can interact with laser light for extended times, laser intensities as low as 100 W/cm^2 are sufficient to drive the two-photon transition. Thus the primary systematic effect of the beam experiments is greatly reduced.

The cold collision frequency shifts of 2S-nS transitions are a potential source of uncertainty. There are no theoretical predictions, and so they will have to be measured. However, if the scattering lengths are comparable to the 1S-2S scattering length the cold collision shift will not be a limiting factor.

The starting point for the proposed experiment is a cloud of cold 2S atoms. The numbers for this look favorable, for more than 10^{10} 2S atoms/s have been produced in the experiments at MIT. A measurement of the metastable lifetime sets an upper limit on the electric fields of in the trap of 20 mV/cm.

A possible setup for the frequency measurement is depicted in Fig. 7. A frequency doubled diode laser at 972 nm is locked to the dye laser at 486 nm, which is the primary laser for driving the 1S-2S transition. A frequency comb generated by a mode locked laser is used to measure the frequency difference between the 972 nm diode laser and the 759 nm laser needed for the 2S-10S transition. Note that this experiment provides its own frequency standard, for the 1S-2S transition serves as the optical frequency reference.

This simple approach to the frequency measurement should allow us to observe other transitions 2S-nS, n=4 and higher. Measuring a series of these transitions should allow sensitive cross checks.

In addition to precision frequency metrology, 2S-nX spectra can provide a wealth of information about scattering lengths for excited atoms. Metatable collision processes, and photoassociation processes, should also be observable. In summary, there are lots of scientific opportunities for trapped ultracold hydrogen.

Acknowledgments

The work would not have been done without the help of the members of the ultra cold hydrogen group at MIT, namely T.J. Greytak, D. Landhuis, S.C. Moss, L. Matos, J. Steinberger and K.M. Vant. The work is supported by the National Science Foundation and the U.S. Office of Naval Research.

References

1. Proceedings of the Symposium *The Hydrogen Atom*, G.F. Bassani, M. Inguscio, and T.W. Hänsch (Eds.): Springer, Heidelberg (1989)

2. For review of the early work on spin-polarized hydrogen see T.J. Greytak and D. Kleppner, in *New Trends in Atomic Physics*, G. Grynberg and R. Stora, (Eds.): North-Holland, Amsterdam, 1984; I.F. Silvera and J.T.M. Walraven, in *Progress in Low Temperature Physics,* D.F. Brewer (Ed.): North-Holland, Amsterdam, 1986, Vol. X; J.T.M. Walraven, in *Quantum Dynamics of Simple Systems*, G.-L. Oppo, S.M. Barnett, E. Riis, and M. Wilkinson, (Eds.): Institute of Physics Publishing, Bristol, 1994
3. C.L. Cesar, D.G. Fried, T.C. Killian, A.D. Polcyn, J.C. Sandberg, I.A. Yu, T.J. Greytak, D. Kleppner, J.M. Doyle: Phys. Rev. Lett. **77**, 255 (1996)
4. E.L. Surkov, J.T.M. Walraven, G.V. Shlyapnikov: Phys. Rev. **A 49**, 4778 (1994); Phys. Rev. **A 53**, 3403 (1996)
5. I.D. Setija, H.G.C. Werij, O.J. Luiten, M.W. Reynolds, T.M. Hijmans, J.T.M. Walraven: Phys. Rev. Lett. **70**, 2257 (1993)
6. J. Doyle, J.C. Sandberg, I.A. Yu, C.L. Cesar, D. Kleppner, and T.J. Greytak: Phys. Rev. Lett. **67**, 603 (1991)
7. D.E. Pritchard, K. Helmerson, A.G. Martin, in: S. Haroche, J.C. Gay, G. Grynberg (Eds.), Atomic Physics 11, World Scientific, Singapore, 1989, p.179.
8. T.C. Killian, D.G. Fried, L. Willmann, D. Landhuis, S.C. Moss, T.J. Greytak, and D. Kleppner: Phys. Rev. **81**, 3807, (1998)
9. D.G. Fried, T.C. Killian, L. Willmann, D. Landhuis, S.C. Moss, D. Kleppner and T.J. Greytak: Phys. Rev. Lett. **81**, 3811, (1998)
10. J.T.M. Walraven: in *Fundamental Systems in Quantum Optics*, J. Dalibard, J.M. Raimond, and J. Zinn-Justin (Eds.), Elsevier Science Publisher B.V., p. 487 (1992)
11. I. A. Yu, J. M. Doyle, J. C. Sandberg, C. L. Cesar, D. Kleppner, T. J. Greytak: Physica B. **194**, 15, (1994)
12. A.I. Safonov, S.A. Vasilyev, I.S. Yasnikov, I.I. Lukashevich, S. Jaakkola: Phys. Rev. Lett. **81**, 4545 (1998)
13. A.P. Mosk, M.W. Reynolds, T.W. Hijmans, J.T.M. Walraven: Phys. Rev. Lett. **82**, 307 (1999)
14. S. Jaakkola, S T. Balkarev, A. A. Haritonov, A. I. Safonov, I. I. Lukashevick: Physica B., **280** 32, (2000)
15. P.W.H. Pinske, A. Mosk, M. Weidenmüller, M.W. Reynolds, T.W. Hijmans, J.T.M. Walraven, C. Zimmermann: Phys. Rev. Lett. **79**, 2423 (1997)
16. D. Kleppner: in *The Hydrogen Atom*, (G.F. Bassani, M. Inguscio, and T.W. Hänsch (Eds.), Springer, Heidelberg (1989)), pp. 103–111
17. see F. Biraben, T.W. Hänsch et al.: *this book*, pp. 17–41
18. Lastest report on the Munich cold hydrogen beam experiment see: M. Niering, R. Holzwarth, J. Reichert, P. Pokasov, Th. Udem, M. Weitz, T.W. Hänsch, P. Lemonde, G. Santarelli, M. Abgrall, P. Laurent, C. Salomon, A. Clairon: Phys. Rev. Lett. **84**, 5496 (2000)
19. C. Schwob, L. Jozefowski, B. de Beauvoir, L. Hilico, F. Biraben, O. Acef, A. Clairon: Phys. Rev. Lett. **82**, 4960 (1999), and references therein
20. S.R. Bramwell, D.M. Kane, A.I. Ferguson: Opt. Comm. **56**, 12 (1985); J.A. Valdmanis, R.L. Fork, J.P. Gordon: Opt. Lett. **10**, 131 (1985); D.M. Kane, S.R. Bramwell, A.I. Ferguson: Appl. Phys. **B 39**, 171 (1986)
21. S.A. Diddams, D.J. Jones, J. Ye, S.T. Cundiff, J.L. Hall, J.K. Ranka, R.S. Windeler, R. Holzwarth, T. Udem, T.W. Hänsch: Phys. Rev. Lett. **84**, 5102 (2000)
22. H. Hess: Phys. Rev. **B 34**, 789 (1986)

23. W.C. Stwalley and L.H. Nosanov: Phys. Rev. Lett. **36**, 910 (1976)
24. J.M. Doyle, J.C. Sandberg, N. Masuhara, I.A. Yu, D. Kleppner, T.J. Greytak: J. Opt. Soc. Am. **B 6**, 2244 (1989)
25. H.F. Hess, G.P. Kochanski, J.M Doyle, N. Masuhara, D. Kleppner, T.J. Greytak: Phys. Rev. Lett. **59**, 672 (1987)
26. R. van Roijen, J.J. Berkhout, S. Jaakkola, J.T.M. Walraven: Phys. Rev. Lett. **61**, 931 (1988)
27. A. Lagendijk, I.F. Silvera, and B.J. Verhaar: Phys. Rev. **B3**, 626 (1986)
28. H.T.C. Stoof, J.M.V.A. Koelman, and B.J. Verhaar: Phys. Rev. **B38**, 4688 (1988)
29. C. Borde: C.R. Hebd. Sean. Acad. Sci. B **282**, 341 (1976); F. Biraben, M. Bassani, B. Cagnac: J. Phys. (Paris) **40**, 445 (1979)
30. C. Cesar, D. Kleppner: Phys. Rev. **A 59**, 4564 (1999)
31. B.J. Verhaar, J.M.V.A. Koelman, H.T.C. Stoof, O.J. Luiten: Phys. Rev. **A 35** 3825 (1987)
32. K. Gibble, S, Chu: Phys. Rev. Lett. **70**, 1771 (1993)
33. S.J.J.M.F. Kokkelmans, B.J. Verhaar, K. Gibble, D.J. Heinzen: Phys. Rev. **A 56**, R4389 (1997)
34. M. Jamieson, A. Dalgarno, J.M. Doyle: Mol. Phys. **87**, 817 (1996)
35. K. Huang: Statistical Mechanics, Wiley & Sons, New York (2nd edn. 1987)
36. M.H. Anderson, J.R. Ensher, M.R. Matthews, C.E. Wieman, E.A. Cornell: Science **269**, 198 (1995); K.B. Davis, M.-O. Mewes, M.R. Andrews, N.J. van Druten, D.S. Durfee, D.M. Kurn, W. Ketterle: Phys. Rev. Lett. **75**, 3969 (1995); C.C Bradley, C.A. Sackett, R.G. Hulet: Phys. Rev. Lett **78**, 985 (1997)
37. For an overview on the research on Bose-Einstein condensation see the BEC-Homepage at Georgia Southern University, http://amo.phy.gasou.edu/bec.html
38. T.W. Hijmans, Y.Kagan, G.V. Shlyapnikov, J.T.M. Walraven: Phys. Rev. **B 48**, 12886 (1993)
39. T.J. Greytak, D. Kleppner, D.G. Fried, T.C. Killian, L. Willmann, D. Landhuis, S.C. Moss: Physica **B 280**, 20 (2000)
40. T.C. Killian: Phys. Rev. A 61, 033610 (2000)
41. L. Willmann, D.G. Fried, D. Landhuis, S.C. Moss, T.C. Killian, D. Kleppner, T.J. Greytak: to be published
42. H-J. Miesner, D.M. Stamper-Kurn, M.R. Andrews, D.S. Durfee, S. Inouye, W. Ketterle: Science **279**, 1005 (1998)
43. M.D. Lee, C.W. Gardiner: Phys. Rev. **A 62**, 033606 (2000)
44. The preliminary analysis of the growth rate for a hydrogen condensate agrees with the expectations for stimulated scattering, S.C. Moss et al.: to be published
45. C. Fertig and K. Gibble: Phys. Rev. Lett. **85**, 1622 (2000)
46. Y. Sortais, S. Bize, C. Nicolas, A. Clairon, C. Solomon, C. Wiliams: Phys. Rev. Lett. **85**, 3117 (2000)
47. B.C. Young, F.C. Cruz, W.M. Itano, J.C. Bergquist: Phys. Rev. Lett. **82**, 3799 (1999)
48. R.J. Rafac, B.C. Young, J.A. Beall, W.M. Itano, D.J. Wineland, J.C. Bergquist: **85**, 2462 (2000)